Journal of
Polymer & Composites
https://journals.stmjournals.com/jopc
ISSN: 2321-2810 (Online)
ISSN: 2321-8525 (Print)
Volume 13, Special Issue 1, 2025
DOI (Journal): 10.37591/JoPC
Research JoPC

Study of Strength of Composite Laminates with Ply-Discontinuities Using FEM

Tanmay Medhekar[1], Rajendra Kumar Gupta[2], Sunil Nimje[3,*]

Abstract

Present research work attempts to understand the effect of ply-discontinuities on the strength of the FRP Composite. Finite Element Analyses have been performed for specimen undergoing four-point bend loading condition using ABAQUS software. Three specimens consisting of different ply sequences, same resin pocket size and location have been considered for the present analysis. Cohesive zone modelling technique is implemented to simulate and predict crack propagation pattern during failure of composite laminate. This technique is used to predict strength and fracture pattern in composite specimens. Results from these Finite Element analyses show that crack will initiate at the interface of the resin pocket and discontinuous ply, and then travels along the length causing delamination of laminate. Flexural strength of the considered laminate has been evaluated through finite element analysis. Subsequently, failure process along with crack propagation pattern has been studied in detail. Suitable ply orientations, for fixed thickness, can be appropriately selected by comparing the strengths of these laminates.

Keywords: GFRP laminate, composite material, CZM, ply-discontinuities, strength of GFRP laminates, stacking sequence

INTRODUCTION

Composite structures are extensively used across various industries today, from automotive to military applications. Manufacturing these structures involves several techniques, including autoclave moulding, pultrusion, Vacuum Assisted Resin Transfer Moulding (VARTM), and Resin Film Infusion (RFI). These methods provide high dimensional accuracy and efficiency. However, for large geometries like boat hulls, turbine blades, sonar domes, and aircraft structures, hand lay-up and VARTM are commonly employed. The latest method for producing large composite structures is the Automated Fibre Placement (AFP) technique, which allows for the production of high-quality large laminates [1]. During AFP, multiple pre-pegs or fibre sheets are laid up in a mould. While this technique enhances accuracy and reduces production time, it may introduce inconsistencies in the laminate, such as gaps and overlaps [1] [2]. These gaps and overlaps modify the geometry of laminate and function as defects when load is applied. These gaps get filled with resin during resin infusion process which gives rise to resin pockets. When the structure is subjected to loading, stress concentration zones are formed at the interfaces of resin pockets and adjacent discontinuous plies [3] [4]. In large structures, repeated resin pockets can significantly weaken the structure. Therefore, evaluating the impact of resin pockets on the strength of composite laminates is crucial.

*Author for Correspondence
Sunil Nimje

[1]M. Tech Student, Department of Mechanical Engineering, Defence Institute of Advanced Technology, Pune, Maharashtra, India
[2]Scientist, Composite Research Centre, Research and Development Establishment (Engr's.), DRDO, Pune, Maharashtra, India
[3]Associate Professor, Department of Mechanical Engineering, Defence Institute of Advanced Technology, Pune, Maharashtra, India

Received Date: March 05, 2024
Accepted Date: June 19, 2024
Published Date: December 06, 2024

Citation: Tanmay Medhekar, Rajendra Kumar Gupta, Sunil Nimje. Study of Strength of Composite Laminates with Ply-Discontinuities using FEM. Journal of Polymer & Composites. 2025; 13(Special Issue 1): S89–S98p.

In the mid-1980s, early research revealed that stress concentration regions form around discontinuities in laminates, functioning as weak links [4]. Beyond these weak regions, stress levels become constant. As long as the weak link regions of two resin pockets do not overlap, the strength of the laminate remains comparable to one with a single resin pocket. Significant research over the last decade has focused on ply-discontinuity and overlapping in laminates, particularly in the aerospace industry's Advanced Grid Structures (AGS). These structures often have overlapping layers that create cross-grid patterns. Behaviour of laminates with discontinuities under flexural and compressive loads can be assessed to develop optimization strategies [5]. Interestingly, in hybrid laminates, discontinuities can control failure mechanisms. For instance, laser-induced discontinuities in a staggered pattern can increase laminate strength because the failed plies continue to carry load post-failure [6]. The effect of discontinuities on laminate strength with open holes varies—positive, negative, or negligible—depending on their position and orientation [2]. In case of In-plane shear strength of laminates, overlap defect was found to be less critical than gaps. These overlaps and discontinuities were found to be completely healed when curing was done with caul plate and were partially healed when caul plate was not used [1]. Subsequent studies used variational analysis to predict the local Young’s modulus of laminates with ply-discontinuities, based on Hashin's method [7]. Researchers have also explored inducing pseudo-ductility in laminates with multiple ply-discontinuities, modifying the geometry to a nacre-like structure, which increases failure strain under flexural loading [3]. When strength is of laminate is considered, studies suggests that ply stacking sequence significantly influences laminate strength. Multi-directional quasi-isotropic laminates exhibit greater impact resistance, while unidirectional laminates show higher flexural strength and modulus [8]. Designing structures that account for these defects requires evaluating their effects through numerical analysis before manufacturing. This can be achieved using software tools that implement cohesive zone modelling in finite element (FE) models to predict progressive failure. UMAT subroutines considering plasticity and damage effects can also predict delamination in laminates with open-hole configurations [9] [10]. This paper studies the technique of using cohesive elements to determine laminate strength and crack propagation patterns. A schematic representation of resin pockets and discontinuous plies is shown in Figure 1.

GEOMETRY AND MATERIAL SPECIFICATIONS

Laminate having 800 mm length and 100 mm width was considered with 12 plies having cured ply thickness of 0.65 mm, this laminate geometry can be understood from Fig. 2. The FE analysis is performed by varying ply sequence as; layup-1: $[0/0/90/90/0/90]_S$, layup-2: $[0/0/90/90/45/45]_S$, layup-3: $[0/0/90/-45/45/90]_S$. Discontinuity (ply-cut) is introduced in bottom two plies, which makes the size of resin pocket as 1.3 mm × 1.3 mm. The specimen was subjected to boundary conditions and loading resembling to Four-point bend test using FE Analysis software ABAQUS. Strength and crack propagation pattern was studied by FE analysis approach. Composite layers and resin pocket are modelled as 3D solid using continuum shell element (SC8R). To simulate the crack initiation and propagation, cohesive zone modelling (CZM) is employed at the interfaces of resin pocket and discontinuous ply as well as in between two plies.

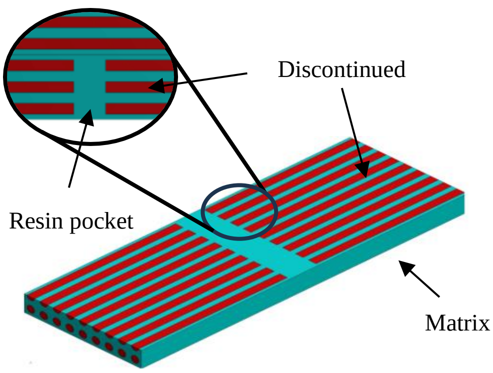

Figure 1. Representation of resin pocket in laminate.

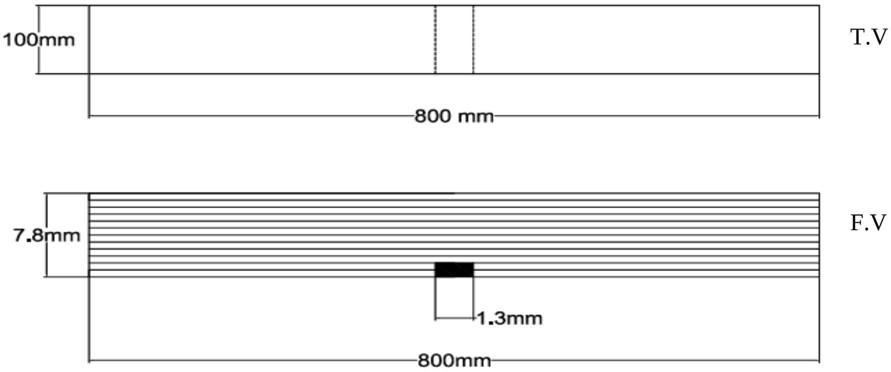

Figure 2. Geometry of laminate

Table 1. Material Properties of GPRF and epoxy.

Material properties	Glass/epoxy laminate	Epoxy
Ply thickness [mm]	0.65	-
E_1, E_2 [GPa]	20.7	3.1
E_3 [GPa]	7.960	-
G_{12}, G_{13}, G_{23} [GPa]	4.15	-
ν_{12}	0.12	0.4
ν_{13}	0.45	
ν_{23}	0.24	
Density [g/cm^3]	1.9 x 10^{-9}	1.1 x10^{-9}

The CZM technique requires modelling of cohesive elements whose behavior is defined as traction-separation response, material parameters needed to be defined are stiffness constants, nominal stress and fracture energy. Theory of these parameters are given in [9] [10] [11]. Material used is Glass Fiber Reinforced Polymer Composite (GFRP) with epoxy as matrix material. The mechanical properties of GFRP and epoxy are given in Table 1.

DEFINING COHESIVE PROPERTIES

The generalized traction-separation equation for cohesive elements is given in Eq.1 [11]. For uncoupled behaviour (normal displacements produces normal stresses only), the non–diagonal elements of stiffness matrix become zero and for coupled behaviour (normal displacements produce normal as well as shear stresses), these elements are non-zero.

$$\begin{Bmatrix} t_n \\ t_s \\ t_t \end{Bmatrix} = \begin{bmatrix} E_{nn} & E_{ns} & E_{nt} \\ E_{ns} & E_{ss} & E_{st} \\ E_{nt} & E_{st} & E_{tt} \end{bmatrix} \begin{Bmatrix} \varepsilon_n \\ \varepsilon_s \\ \varepsilon_t \end{Bmatrix} \quad (1)$$

In Eq. 1, subscripts *n, s* and *t* indicate the *normal* and *two shear directions* respectively and *t, E* and *ε* represent *traction, stiffness and strain (displacement)* respectively. User has to decide whether the stiffness matrix (matrix E in Eq.1) will be coupled or uncoupled based on the mode of fracture estimated. For cohesive elements, the mode of fracture depends on the relative movement of the top and bottom surfaces on cohesive element. In this study, estimated mode of fracture is mode-I. The stiffness constants are defined as elastic traction-separation law. Under this law the cohesive element behaves linearly until the damage initiation criterion is satisfied. The damage initiation criterion used in this study is Quadratic Stress Damage Initiation or Quads damage in the software, represented by Eq. 2.

$$\left\{\frac{\langle t_n\rangle}{t_n^0}\right\}^2 + \left\{\frac{t_s}{t_s^0}\right\}^2 + \left\{\frac{t_t}{t_t^0}\right\}^2 = 1 \quad (2)$$

In Eq. 2, the terms t_n^0 , t_s^0 and t_t^0 represents *peak stress* values along *normal* and *two in-plane shear directions* respectively, which are to be specified. When this equation is satisfied, the damage is considered to be initiated. This is followed by damage evolution criterion. Damage evolution law states the rate at which stiffness of material will be degraded from the point where damage initiation criterion is satisfied. A scalar damage variable '*D*' is considered, which represents combined effect of every active damage mechanism in model. The initial value of this variable is '0' and it monotonically increases to '1' as the loading is increased. Energy based and strain-based damage evolution criterion are available in software. In this study energy-based damage evolution criterion is used, which uses fracture energy of all three fracture modes to determine rate of damage. Composites mostly undergo a mixed-mode failure, that all three fracture modes (mode-I, mode-II and mode-III) co-exists during failure [9]. A lot of work was done to find the mixed-mode behaviour suitable for composites. Power law and Benzeggagh – Kenane (BK) criterion were found to be suitable as they take into account all three fracture energies. Although for simplicity it is assumed that mode-II and mode-III fracture energies are equal as both failures occur due to shear loadings. Here, power law is used because it has capability to consider different mode-II and mode-III energies. The power law equation used by ABAQUS is given in Eq. 3.

$$\left\{\frac{G_n}{G_n^C}\right\}^\alpha + \left\{\frac{G_s}{G_s^C}\right\}^\alpha + \left\{\frac{G_t}{G_t^C}\right\}^\alpha = 1 \quad (3)$$

In eq. (3), G_n^c , G_s^c and G_t^c represent critical fracture energies needed to cause failure along mode- I, II and III directions respectively such that when this equation is satisfied, total energy released during failure (G^c) = G_T = G_n + G_s + G_t. G_n^c , G_s^c and G_t^c are material properties needed to be specified. $\propto = 1$ or 2 is mostly used with power law, in this work $\propto = 1$ is found to be suitable to predict the failure.

SELECTION OF SOLVER

ABAQUS uses two types of solving methods Implicit method which is good for solving linear and non-linear models undergoing static and quasi-static events. Another is explicit method which is good for highly non-linear models involving high strain rates. Implicit solver requires large number of iterations to achieve convergence of solution, whereas explicit solver does not need convergence but needs a very small time-step for stability. Studies show that explicit analysis is more useful in predicting strength of laminate with CZM technique than the implicit analysis [12]. CZM technique requires softening behaviour and stiffness degradation of material which causes serious convergence issues in implicit solver even with viscous regularization and very small time-step. Properties of cohesive material are taken from literature [13] given in Table 2.

Table 2. Properties of cohesive elements.

Stiffness constant [N/mm^3]			Failure stresses [MPa]			Fracture energies [N/mm]		
E_{nn}	E_{ss}	E_{tt}	σ_{1max}	σ_{2max}	σ_{3max}	G_{Ic}	G_{IIc}	G_{IIIc}
4.67×10^5	1.67×10^5	1.67×10^5	60	82.6	82.6	0.2	1	1
Type = Energy			Mixed – Mode behaviour = Power LawPower [∝] = 1			Density = 1.3×10^{-11} [g/cm^3]		

BOUNDARY CONDITIONS

Boundary conditions were chosen according to criterion mentioned in ASTM D7264/ D7264M. The support span and loading span was chosen to be 600 mm and 300 mm respectively. Free body diagram of beam subjected to four-point bend loading is given in Fig. 3. For simplicity and to reduce the error caused due to rollers, the boundary conditions and loading are applied on the node sets created during meshing. Loading was applied as displacement to load node set with rate of 4mm/min [14-22].

Journal of Polymer & Composites
Volume 13, Special Issue 1
ISSN: 2321-2810 (Online), ISSN: 2321-8525 (Print)

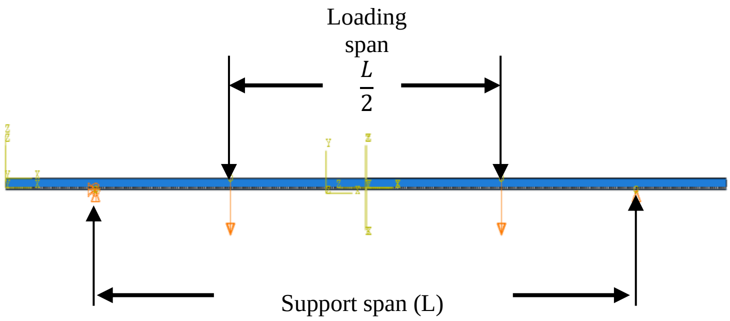

Figure 3. Four-point bend loading conditions.

MESHING

Different mesh sizes were used to model cohesive layer and composite and rein pockets. Finer mesh size of 0.325mm was used for cohesive layers and resin pocket. Mesh size of 2 mm is employed for composite. Continuum Shell (SC8R) element type is used for composite and resin pocket and Cohesive (COH3D8) element type for cohesive layers is implemented.

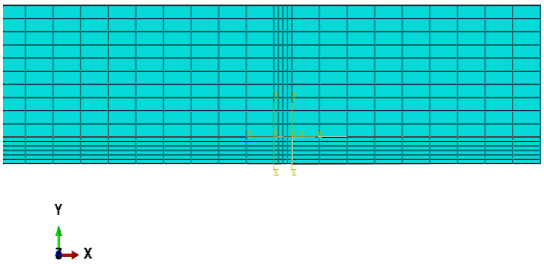

Figure 4. Meshing scheme.

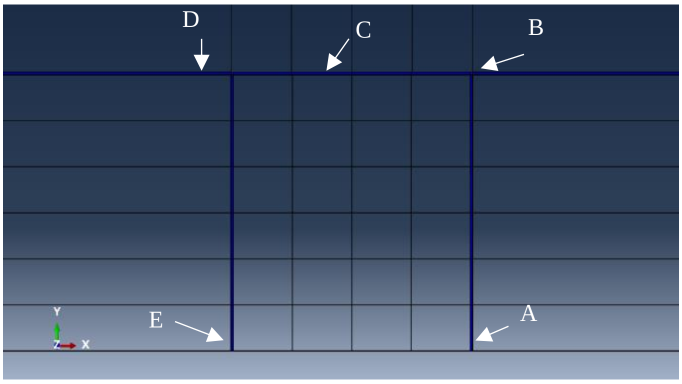

Figure 5. Interface points.

RESULTS AND DISCUSSION

Results of FE analysis shows the Von-Mises stress variation in cohesive elements of laminate. Interface points are shown in Figure 5. Stress variation at these points with respect to time is shown in Figure 6. Here, in layup-1, Figure 6(a), it is observed that cohesive elements along the right interface of resin pocket and ply fails first which gives rise to crack. This crack then propagates along this interface towards point B which fails after point A. Crack reaches points B and C simultaneously showing crack travelled in both directions at same time keeping left interface of resin pocket intact. Crack reaches point D much after it has passed point B. Crack travels along the length after point B indicating delamination. Figure 7 represents the sequence of failure of cohesive elements of layup-1. As the crack propagates delamination between the plies and resin pocket separation is observed.

Figure 6 (b) & (c) show the same for layup-2 & layup-3 respectively. In Figure 6 (b) it can be seen that cohesive elements at point A and E fail simultaneously exhibiting similar behaviour, indicating crack initiates at left and right interfaces of resin pocket simultaneously. But there is some gap between failure points of B and D, suggesting that crack starts propagating along length from point B resulting in delamination. Figure 8 represents failure sequence in layup-2.

Stress variation in cohesive elements of layup-3 exhibits completely different behaviour compared to other two layups. In layup-3, crack initiates along the right interface of resin pocket and travels along this interface then resulting in delamination from the right side of pocket, as observed in Figure 6(c). At same time another crack initiates along left interface of pocket. First crack then travels along top surface of resin pocket which separates it from laminate. Second crack then travels along its interface resulting in delamination from left side of pocket. Figure 9 represents failure sequence in layup-3. As load is increased, four stages of crack propagation, (a) Pre-crack stage, (b) crack initiation stage, (c) crack propagation stage and (d) Final crack stage can be observed in Figure 7-9. By combining Figure 5 and results shown in Figure 6-9, failure mechanism of laminate under flexural load can be studied.

The load-deflection curve of all layups is different as the failure patterns are different. The dips in the curve represent the failure of cohesive elements, this is because when cohesive elements fail the bond between the continuous plies and ply cuts breaks which results in change in the load bearing capacity of laminate, this failure is observed in Figure 7-9. Also, there is difference between laminates with ply-cuts and that without ply-cuts, with respect to maximum load carried by a laminate having same ply sequence. This difference in load capacity can be observed from Figures.10-12. Maximum load sustained by laminate before and corresponding strength (according to ASTM D7264) is mentioned in Table 3.

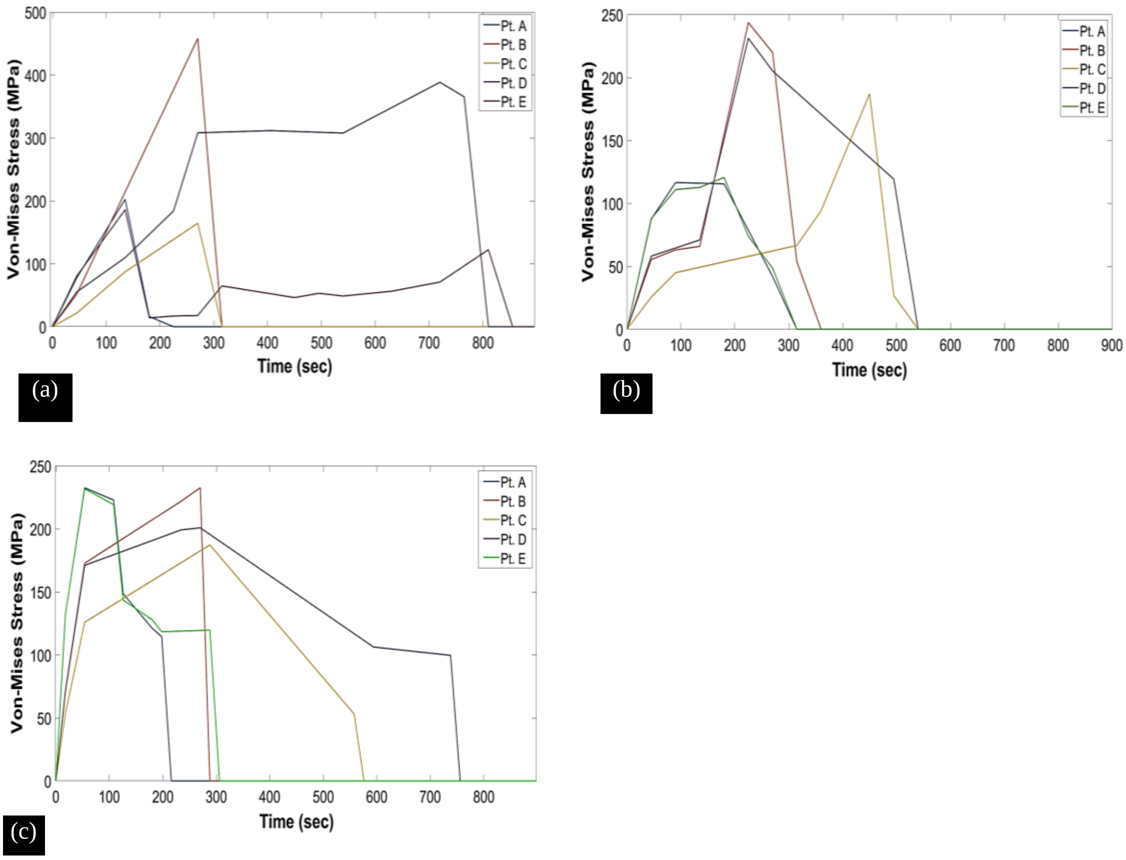

Figure 6. Stresses in Cohesive Elements, (a) layup-1, (b) layup-2, (c) layup-3.

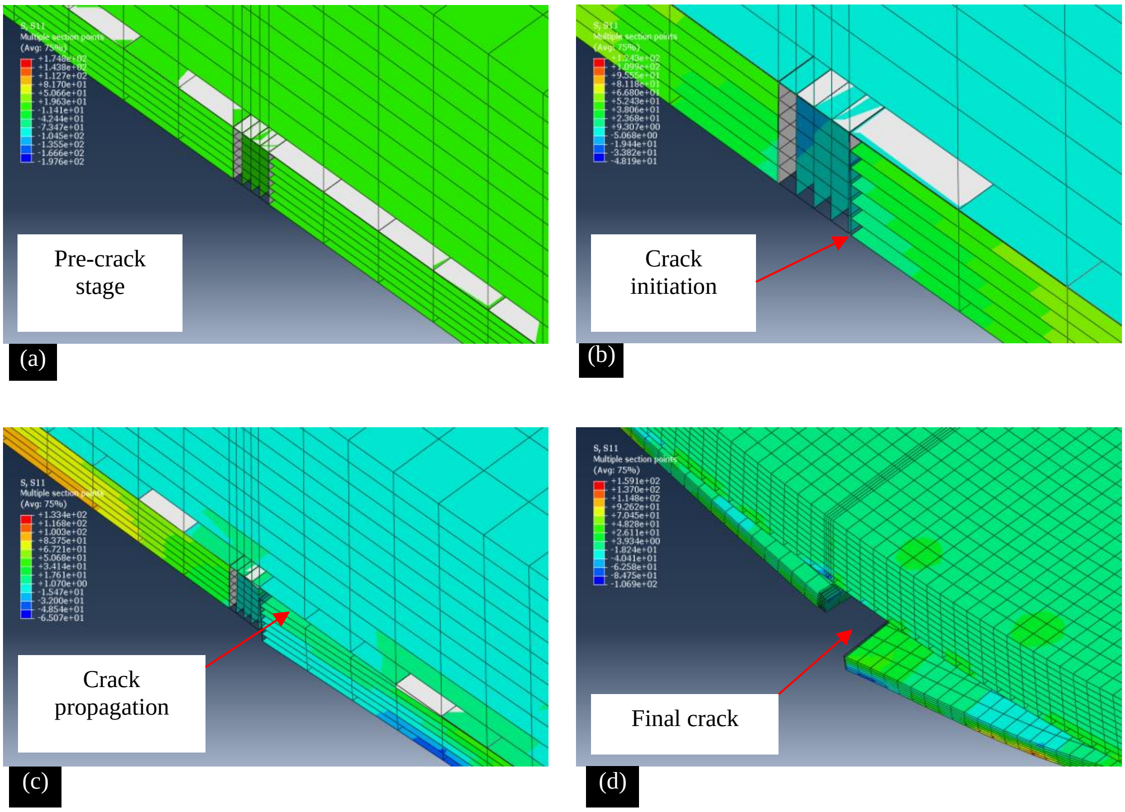

Figure 7. Stress (σ11) contour during crack propagation in layup-1.

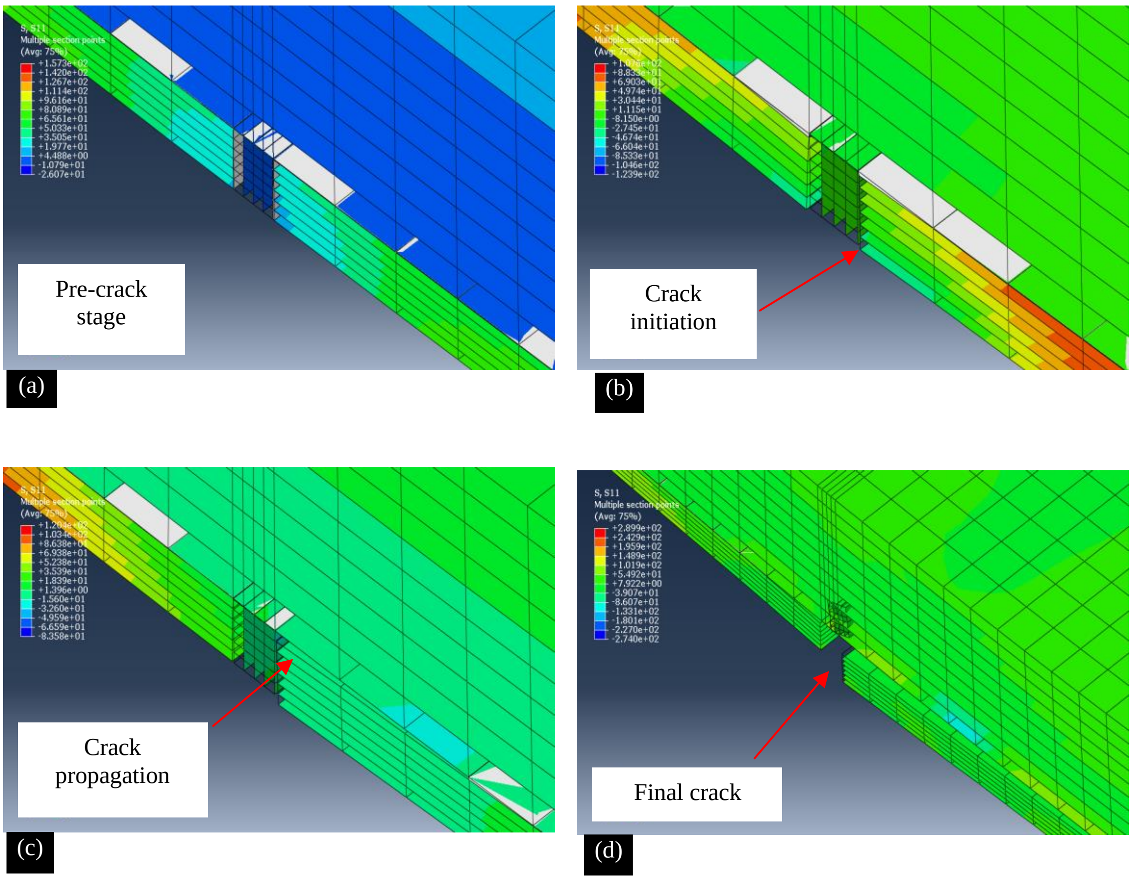

Figure 8. Stress (σ11) contour during crack propagation in layup-2.

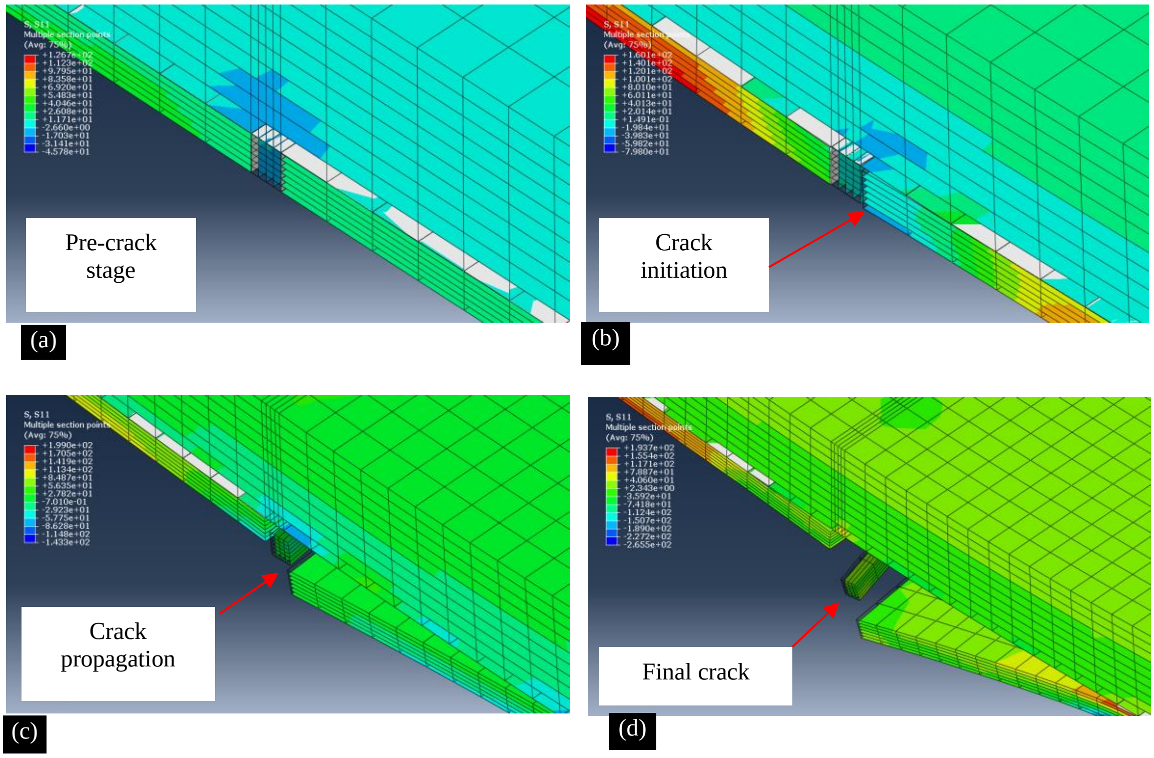

Figure 9. Stress (σ11) contour during crack propagation in layup-3.

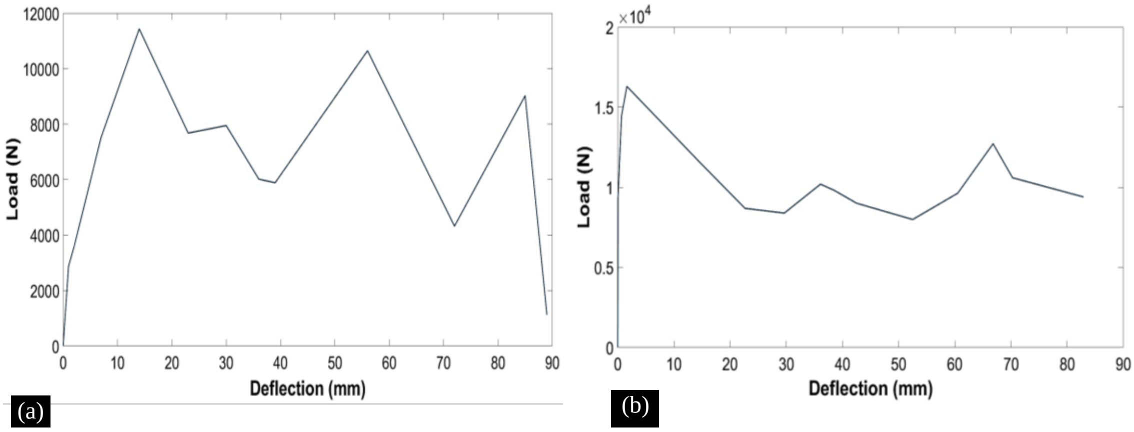

Figure 10. Load vs Deflection of Layup-1, (a) with ply-cut, (b) without ply-cut.

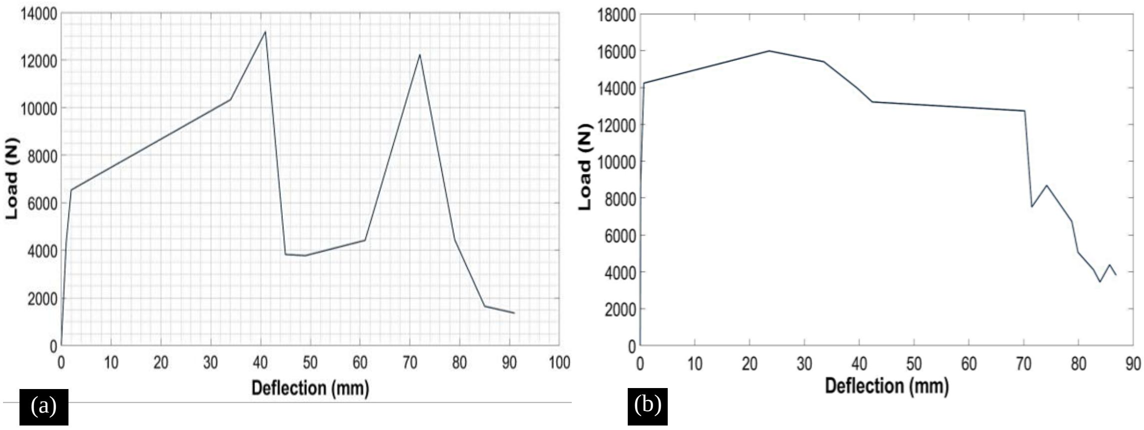

Figure 11. Load vs Deflection of Layup-2, (a) with ply-cut, (b) without ply-cut.

Journal of Polymer & Composites
Volume 13, Special Issue 1
ISSN: 2321-2810 (Online), ISSN: 2321-8525 (Print)

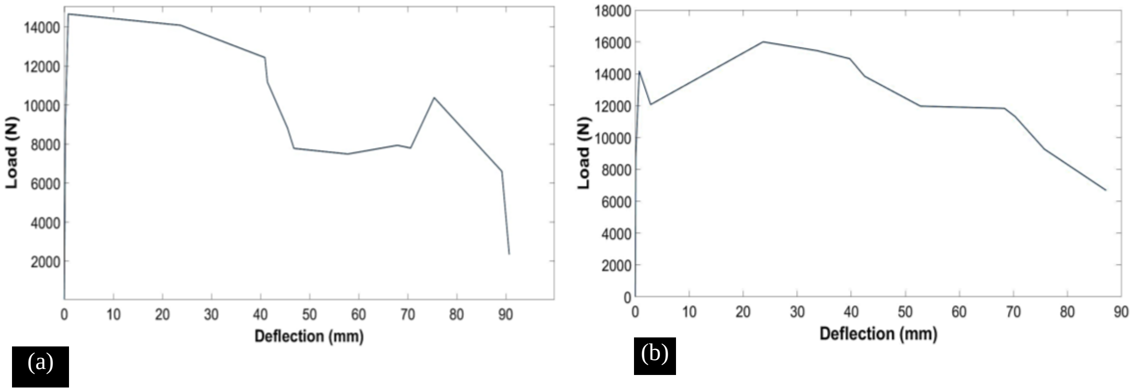

Figure 12. Load vs Deflection of Layup-3, (a) with ply-cut, (b) without ply-cut.

Table 3 shows considerable decrease in strength of laminate due to presence of discontinuity. For layup-1 the strength deceased from 16297.6 N to 11432.3 N for resin pocket with considered size. Same phenomenon is with layups-2 and 3, with decrease in strength from 15981.2 N to 13196.3 N and 15996.6 N to 14650.4 N respectively. So, strength is decreased by 29.85%, 17.42% and 9.18% for layup-1, 2 and 3 respectively.

Table 3. Maximum Load Sustained and Strength of laminates.

Layups		**Max Load Sustained (N)**		**Strength (MPa)**	
		Ply-cut	***No ply-cut***	***Ply-cut***	***No ply-cut***
1.	[0/0/90/90/0/90]s	11432.3	16297.6	845.58	1205.44
2.	[0/0/90/90/45/45]s	13196.3	15981.2	976.06	1182.04
3.	[0/0/90/-45/45/90]s	14650.4	15996.6	1083.60	1183.18

CONCLUSION

Cohesive Elements are successfully employed to simulate the crack propagation pattern in layered composite laminate. Failure of cohesive elements can be seen by sudden dip in stress levels. By observing sequence of these dips at different points, crack propagation pattern can be studied. The effect of ply-discontinuity on the strength of laminate has been evaluated. For the presented layup configuration, load, and ply-cut, the strength reduction due to ply discontinuity varies from 9.18% to 29.85%. This indicates that strength reduction is also dependent on the layup sequence.

From these results, it is seen that the least reduction in strength is shown by layup-3, this is because layup-3 has both $\pm 45^0$ ply-orientation which can sustain more flexural loads after failure of bottom two 0^0 plies which contained ply-discontinuity. Layup-3 is stronger compared to layup-2 which has only $+45^0$ plies. The unidirectional laminate undoubtedly exhibits superior flexural strength compared to the layups examined above, however, it lacks adequate transverse strength. Therefore, to bolster the laminate's transverse strength, plies oriented at ±45° can be imperative additions. Hence it can be concluded that for a given thickness and to withstand flexural loads, the layup of laminate should contain $\pm 45^0$ orientation plies, also this orientation is optimum orientation between 0^0 and 90^0 orientation as it will provide optimum strength against tensile loads along global X and Y-directions as well as unpredictable impact loading.

NAME, DESIGNATION AND AFFILIATION OF AUTHORS

1. Tanmay Medhekar, Student, Defence Institute of Advanced Technology, Pune, India, 411025.
2. Rajendra Kumar Gupta, Scientist F, Research and Development Establishment (Engr's.), DRDO, Pune, India, 411015
3. 3*Sunil Nimje, Associate Professor, Defence Institute of Advanced Technology, Pune, India, 411025ORCID: [1]0009-0000-3279-558X, [2]0000-0002-7878-9713, [3]000-0002-0068-8605

REFERENCES

1. D. C. P. D. C. B. Marine Lan, " Influence of embedded gap and overlap fiber placement defects on the microstructure and shear and compression properties of carbon–epoxy laminates," Composites: Part A, pp. 198-207, 2016.
2. P. L. R. B. Aymen Marouene, "Experimental and numerical investigation on the open-hole compressive strength of AFP composites containing gaps and overlaps," Composite Materials, pp. 3631-3646, 2017.
3. M. Y. I. P. B. R. S. T. R. Malkin, "Ductility in composites: Influence of ply-cuts on the flexural behaviour of CFRP," Research Gate, 2011.
4. R. Y. Darby, "Effect of discontinuous plies on tensile strength of CFRP laminate," Journal of materials science Letter, 1985.
5. M. J. D. B. G. P. J. X. Cong Zhao, "Influences of ply waviness and discontinuity on automated fibre placement manufactured grid stiffeners," Composite Structures, p. 113106, 2021.
6. A. A. Y. S. G. B. S. T. P. Jun Tang, "Staggered ply discontinuities for tailoring the tensile behavior of hybrid carbon fiber/self-reinforced polypropylene composites: A study of pattern parameters," Composites Part A, p. 105551, 2019.
7. V. V. S. O. M. J. M Fikry, "Analytical prediction of local young's modulus in CFRP with ply discontinuities," Advanced composite materials, pp. 843-865, 2023.
8. S. R. M. Z. S. E. R. O. Ogunlele, "The Influence of Ply Stacking Sequence on Mechanical Properties of Carbon/Epoxy Composite Laminates," MDP, 2022.
9. E. V. M. K. S. J-F Chen, "Simulating progressive failure of composite laminates including in ply delamination effect," Composites Part A, pp. 185-200, 2014.
10. B. M. A. Chakrabarti, "Elasto-plastic damage model considering cohesive matrix interface layers of laminate," Journal of Mechanical Science and Technology, pp. 121-127, 2017.
11. "Dassault Systemes 2017 Abaqus/cae user guide," [Online]. Available: https://help.3ds.com/2017/English/DSSIMULIA_Established/SIMACAEELMRefMap/simaelm-m-CohesiveElements-sb.htm?contextscope=all&id=f6297fb7c60945aa9b916c9684cda01e&_gl=1*1awefs6*_up*MQ..*_ga*MTEyMzkxNDU4OC4xNzE1NTI1OTIw*_ga_DYJDKXYEZ4*MTcxNTUyNTkyMC4xLjAuMTcx.
12. J. Swinnen, "Modelling FRP open-hole tensile tests in Abaqus," Delft, 2018.
13. S. R. H. M. R. W. K W Gan, "Measurement and modelling of interlaminar shear strength enhancement under moderate through-thickness compression," Composites Part A, pp. 18-25, 2013.
14. J. M. R. B. Y. M. I Darby, "Effect of discontinuous plies on tensile strength of CFRP laminate," Journal of materials science Letter, pp. 203-206, 1985.
15. M. R. W. Z. Petrossian, "Parametric study of delamination in composites with discontinuous plies using analytical solution based on fracture mechanics," Composites part A, pp. 403-414, 1997.
16. J.-H. C. R-H Maa, "A CDM based failure model for predicting strength of notched composite lamiantes," Composites Part B, pp. 479-489, 2002.
17. M. I. T. S. S. F. M. R. A. S Huzni, "Finite element model of delamination process on composite laminate using cohesive elements," International Journal of Automotive and Mechanical Engineering, pp. 1023-1030 , 2013.
18. M. J. M. R. W. G Czel, "Demonstrations of pseudo-ductility in multidirectional hybrid composite made of discontinuous carbon/epoxy and continuous plies," Composites Part A, 2015.
19. Z. N. A. S. O. M. J. M Fikry, "Mechanical properties and damage behaviour of angle ply CFRP laminates with discontinuous plies," AIP conference, 2020.
20. E.-G. N. P Hale, "Three-point bending analysis with cohesive surface interaction for improved delamination," Modelling and simulation in materials science and engineering, p. 035007, 2020.
21. C. W. Falk Heinecke, "Manufacturing-Induced Imperfections in Composite Parts Manufactured via Automated Fiber Placement," Composite Science, 2019.
22. ASTM D7264, Standard test method for flexural properties of polymer matrix composite materials.

